HHS Public Access

Author manuscript

*Laryngoscope*. Author manuscript; available in PMC 2015 October 01.

Published in final edited form as:

*Laryngoscope*. 2014 October ; 124(10): 2321–2326. doi:10.1002/lary.24707.

# A rabbit vocal fold laser scarring model for testing lamina propria tissue engineering therapies

**Ted Mau, MD, PhD**, **Mindy Du, BS**, and **Chet C. Xu, PhD**

Department of Otolaryngology-Head and Neck Surgery, University of Texas Southwestern Medical Center, Dallas, Texas, U.S.A

## Abstract

**Objectives/Hypothesis—**To develop a vocal fold scarring model using an ablative laser in the rabbit as a platform for testing bioengineered therapies for missing or damaged lamina propria.

**Study Design—**Prospective controlled animal study.

**Methods—**An optimal laser energy level was first determined by assessing the depths of vocal fold injury created by a Holmium:YAG laser at various energy levels on fresh cadaveric rabbit larynges. The selected energy level was then used to create controlled unilateral injuries in vocal folds of New Zealand white rabbits, with the contralateral folds serving as uninjured controls. After 4 weeks, the larynges were harvested and subjected to excised-larynx phonation with high-speed imaging and immunohistochemical staining for collagen types I and III, elastin, and hyaluronic acid (HA) with quantitative histological analysis.

**Results—**1.8 joules produced full-thickness injury of the lamina propria without extensive muscle injury. After 4 weeks, the injured vocal folds vibrated with reduced amplitude ($P = 0.036$) in excised-larynx phonation compared to normal vocal folds. The injured vocal folds contained a higher relative density of collagen type I ($P = 0.004$), higher elastin ($P = 0.022$), and lower HA ($P = 0.030$) compared to normal controls. Collagen type III was unchanged.

**Conclusions—**With its potential for higher precision of injury, this laser vocal fold scarring model may serve as an alternative to scarring produced by cold instruments for studying the effects of vocal fold lamina propria bioengineered therapies.

**Level of Evidence—**N/A.

### Keywords

vocal fold scarring; lamina propria; laser injury; collagen; hyaluronic acid; high speed imaging; excised larynx

Send correspondence to: Ted Mau, MD PhD, Department of Otolaryngology-Head and Neck Surgery, UT Southwestern Medical Center, 5323 Harry Hines Blvd, Dallas, Texas 75390, Phone: (214) 648-2042, Fax: (214) 648-9122, ted.mau@utsouthwestern.edu.

Conflict of Interest: None.

This work has been accepted for oral presentation at the 135th Annual Meeting of the American Laryngological Society in Las Vegas on May 15, 2014.

Financial Disclosure: This work was supported by NIDCD grant R03 DC011145. The content is solely the responsibility of the authors and does not necessarily represent the official views of the National Institute On Deafness And Other Communication Disorders or the National Institutes of Health.

## INTRODUCTION

Vocal fold scarring is a significant cause of poor voice quality following vocal fold injury.[1] The development of novel therapies for the prevention and treatment of vocal fold scarring has been the focus of intense investigation for well over a decade. Current tissue engineering approaches encompass cell-based therapy, growth factor modulation, and the development of extracellular matrix (ECM) scaffolds.[2,3] Animal models have been critical to the process of evaluating the functional performance of these therapies *in vivo*.[4] The rabbit has been heavily utilized because of the similarities of its vocal fold microstructure to that of human vocal folds, the relative accessibility of its vocal folds to surgical manipulation, its inherent non-vocal nature, and lower cost compared to larger species.[5] Previously reported methods to create vocal fold injury in the rabbit include cupped-forcep biopsies[6,7], vocal fold stripping[8], laser ablation[9], and microflap incision.[10] In some cases the injury extended to the cartilaginous glottis or deep into muscle.[9,11] As most current research in vocal fold tissue engineering focuses on regeneration of the lamina propria, it would be advantageous to have an injury model where the injury depth is largely confined to the lamina propria, does not involve total loss of the lamina propria, simulates vocal fold injuries in humans, and can be created with precision in a graded manner.

We present a pilot study to establish the feasibility of a vocal fold injury model in the rabbit using a holmium:YAG (Ho:YAG) laser. The Ho:YAG laser operates at a characteristic wavelength of 2100 nm with water as the target chromophore. It has been used in a variety of otolaryngologic procedures, including airway surgery.[12,13] We sought to take advantage of its ability to deliver quantized energy through a sub-millimeter diameter fiber to create defined ablative wounds. The objectives of this study were: 1) to demonstrate the feasibility of creating controlled vocal fold injury using the Ho:YAG laser in a rabbit model, and 2) to characterize the lamina propria deficit created in this model. We hypothesized that the laser injury would result in lamina propria deficit without gross damage to the underlying muscle. The overall goal is to establish a vocal fold scarring model as a platform for testing novel bioengineered lamina propria regenerative therapeutics.

## MATERIALS AND METHODS

### Determination of Optimal Laser Energy Level

A preliminary study was carried out to determine the optimal laser energy level using intact cadaveric larynges from 3 rabbits sacrificed for unrelated experiments. The larynges were harvested immediately post-mortem and the laser treatment performed shortly after. The Ho:YAG laser (Lumenis VersaPulse PowerSuite, 2.1 μm) at 600 mJ/pulse was delivered via a 365-micron fiber. Laser treatment was performed in contact mode, i.e. the fiber tip just touching the vocal fold surface but not pressing into the mucosa. One vocal fold in each larynx was treated, while the other served as control. The experimental vocal fold was treated at 3 spots along the membranous vocal fold: one just anterior to the vocal process, one at the mid-membranous vocal fold, and one just short of the anterior commissure. These 3 spots were approximately equidistant. In the first larynx, 1 pulse was applied at each spot (0.6 J). In the second larynx, 3 pulses were applied at each spot (1.8 J). In the third larynx, 5

pulses were applied at each spot (3.0 J). The larynges were then fixed in formalin for histologic processing.

## Animals and Surgical Procedure

The experimental protocol was approved by the Institutional Animal Care and Use Committee (IACUC) of UT Southwestern Medical Center, in accordance with the U.S. Public Health Service Policy on Humane Care and Use of Laboratory Animals, the NIH Guide for the Care and Use of Laboratory Animals (NIH Publication #85-23 Rev. 1985), and the Animal Welfare Act (7 U.S.C. et seq.). Eight New Zealand white rabbits weighing 2.8 to 3.4 kg underwent direct laryngoscopy during which laser injury was created on one vocal fold (detailed below), with the other side serving as control. General anesthesia was induced with intramuscular administration of ketamine (35 mg/kg) and xylazine (3 mg/kg). Buprenorphine (0.02 mg/kg) was administered after induction and prior to laryngoscopy. Heart rate, temperature, respiratory rate, and oxygen saturation level were monitored. Suspension laryngoscopy was performed with a No.1 Miller blade. Vocal fold intervention was performed under visual guidance using a 2.7-mm, 30-degree Hopkins telescope. 4% lidocaine was dripped onto the arytenoids prior to laser application. The Ho:YAG laser at 600 mJ/pulse was delivered via a 365-micron fiber. Laser treatment was performed in contact mode. The laser fiber was threaded through a 20G spinal needle and directed to the membranous vocal fold (Fig. 1). For each animal, one vocal fold was treated, while the other served as uninjured control. The experimental vocal fold was treated at 3 spots along the membranous vocal fold: one just anterior to the vocal process, one at the mid-membranous vocal fold, and one just short of the anterior commissure (Fig. 1). These 3 spots were approximately equidistant. At each spot, 3 pulses were delivered, for 1.8 J per spot, or 5.4 J per vocal fold. The animal was then recovered.

## Excised Larynx Phonation, High-Speed Imaging and Videokymography

Four weeks after laser injury, the animals were sacrificed and their larynges harvested. Four of the eight larynges were subjected to excised larynx phonation, which was induced as previously described.[14] Subglottal airflow was slowly increased until audible phonation occurred. As soon as phonation began, high-speed imaging data were acquired at 6000 frames per second using a Phantom V311 high speed camera (Vision Research, Wayne, NJ) and Nikkon micro lens (Nikkon, Melville, NY) mounted over the larynx. The videos were inspected to identify the earliest segment of stable vibratory behavior following phonation onset. Videokymographic images were generated by custom software from a transverse line taken from the high-speed images at the location of the greatest amplitude during vocal fold vibration, which is typically at the mid-membranous vocal fold. The videokymographic images were then manually analyzed using ImageJ (NIH, Bethesda, MD) to measure the amplitude of vibration, defined as the difference between the vocal fold edge position at the maximum opening and closing phases of vibration.

## Histology and Immunohistochemistry

The larynges were fixed in 10% formalin, decalcified in 0.35M EDTA, then embedded in paraffin for sectioning. Successive 5.0-μm thick coronal sections of the laryngeal specimens were prepared. Hematoxylin and eosin (H&E) staining was performed using standard

methods. Immunohistochemical (IHC) stainings for collagen type I, collagen type III, elastin, and hyaluronic acid (HA) were carried out as previously described.[15,16] For collagen type I, collagen type III, and elastin, sections were incubated in Proteinase K (Sigma, St. Louis, MO) epitope retrieval buffer for 15 minutes at 37°C, then incubated in Pierce peroxidase suppressor solution (Thermo Fisher Scientific, Rockford, IL), followed by 5% bovine serum albumin (BSA; Sigma, St. Louis, MO) blocking buffer with serial washings in between. Biotinylated anti-collagen type I antibody (Millipore, Billerica, MA), anti-collagen type III antibody (MP Biomedicals, Santa Ana, CA), anti-elastin antibody (Millipore, Billerica, MA), and biotinylated hyaluronic acid binding protein (HABP; Calbiochem, San Diego, CA) were applied overnight at 4°C or for 4 hours at 37°C. After unbound primary antibodies were washed off, sections were incubated with horseradish peroxidase (HRP)-conjugated streptavidin (for collagen type I and HA; Thermo Fisher Scientific, Rockford, IL) or anti-mouse IgG-peroxidase secondary antibody (for collagen type III and elastin; Sigma, St. Louis, MO) at room temperature for 1–1.5 hours. The sections were then incubated with Pierce metal enhanced diaminobenzidine (DAB) peroxidase substrate solution (Thermo Fisher Scientific, Rockford, IL) for 2 minutes. Epiglottic tissue served as positive controls. Laryngeal sections with the primary antibody replaced by BSA were used as negative controls.

### Quantitative Histological Analysis

Histological and IHC images were captured with a Leica DM200 microscope (Bannockburn, IL) and a MicroFire microscope CCD digital camera (Optronics, Goleta, CA). The relative densities of collagen type I, type III, elastin, and HA were estimated from their staining intensities and relative areas as previously described in detail[15,16] and briefly summarized here. Color images were first converted to 8-bit grayscale images in Photoshop (Adobe, San Jose, CA). For each grayscale image, visual comparisons were made with its corresponding H&E stained image in order to select lower and upper threshold values so that pixels representing areas of the molecule of interest can be clearly visualized with minimal background. Pixels with intensities bracketed by the thresholds were deemed representative of the molecule of interest. The relative density of the molecule of interest was then calculated as the fraction of the positively stained area to the total area of the vocal fold lamina propria using Image J.

### Statistical Analysis

Paired Student's *t* tests were applied to vibrational amplitudes from high-speed imaging and the relative densities on histology and IHC staining, with alpha = 0.05.

## RESULTS

### Laser Injury

An intraoperative photo is shown in Figure 1. Figure 2 shows the extent of injury created by the Ho:YAG laser at various energy levels in fresh cadaveric rabbit larynges. At 0.6 J, only the epithelium and part of the lamina propria were disrupted (Fig. 2A). At 1.8 J, the ablation extends through the lamina propria to the superficial part of the muscle (Fig. 2B). At 3.0 J, a

large muscle deficit was produced (Fig. 2C). Based on these results, 1.8 J was chosen for the survival experiments.

### Histology and IHC Staining

Figure 3 shows representative coronal sections of the larynx harvested 4 weeks after laser treatment. Collagen type I, localized to the deeper aspect of the lamina propria in the normal vocal fold (Fig. 3B, right), is present through the entire thickness of the lamina propria in the scarred vocal fold (Fig. 3B, left). There is no appreciable difference in the morphological distribution of collagen type III and elastin between normal and scarred vocal folds (Fig. 3C, D). HA, which can be seen as a continuous band in the lamina propria extending from the supraglottis to the subglottis in the normal vocal fold (Fig. 3E,F, right), is noticeably deficient at the location of the laser injury in the scarred vocal fold (Fig. 3E,F, left).

The relative densities of select ECM constituents in IHC staining are plotted in Figure 4. Collagen type I was present at higher levels in the scarred vocal folds ($P = 0.003$). Collagen type III density was similar between normal and scarred vocal folds. Elastin was higher in scarred vocal folds ($P = 0.022$), while HA was lower in the scarred vocal folds ($P = 0.030$).

### High-Speed Imaging and Videokymography

A representative videokymograph from excised larynx phonation is shown in Figure 5. The scarred vocal folds vibrated with a mean amplitude of 0.18 mm (SD = 0.02 mm), while the control vocal folds vibrated with a mean amplitude of 0.31 mm (SD = 0.10 mm). This difference was statistically significant ($P = 0.036$, n=4).

## DISCUSSION

Small animal models such as the rabbit or rat[17] have been indispensible in the development of novel tissue engineering therapies for damaged or missing vocal fold lamina propria. A well-established experimental paradigm consists of the intentional creation of a vocal fold wound preceded or followed by the therapeutic intervention. However, the much smaller size of the animal larynx often precludes the degree of precision that is possible in human vocal fold surgeries. While vocal fold microflap elevation has been demonstrated in the rabbit,[10] it is not meant as a way to create scar, and vibratory function returns to normal within a week.[18] Cupped forceps biopsy, which is a well-accepted vocal fold injury method in animal models, in theory could limit the size of the mucosal defect to the size of the cup. In our experience, the mucosal defect tends to be larger than the cup size, because the rabbit vocal fold mucosa is highly elastic and the defect is created by a ripping rather than cutting action. Even a relatively small cup size, e.g. 1 mm, is far greater than the thickness of the lamina propria (e.g. Fig. 2). These vocal fold injury methods in small animal models may produce an exaggerated wound healing response relative to lamina propria scarring in humans, a concern that has been raised before.[19,20] The present work is an attempt to establish a vocal fold scarring model where the extent of injury can be controlled with some precision. The intent is to generate a response that primarily reflects injury to the lamina propria rather than injury to the muscle underneath.

We chose to examine the histologic and vibratory responses at 4 weeks post-injury in this pilot study for several reasons. Gene expression levels of inflammatory cytokines have been shown to return to baseline by 21 days following cupped forcep biopsy of rabbit vocal folds.[21] Similarly, histological features of rat vocal folds recovered to normal at 1 month following PDL laser irradiation.[22] By 4 weeks, the inflammatory and proliferative phases of wound healing are complete, and the wound should be in the remodeling phase, which is thought to start by week 3.[23] Our findings at 4 weeks after injury should therefore reflect scarring and not the reparative process that would have restored normal tissue architecture within the first 2–4 weeks.

Collagen type I is sparse in normal vocal folds and is upregulated in response to injury. Its level peaks at day 5 following vocal fold injury in a rat model, declines after 8 weeks, but remains elevated above uninjured controls through 12 weeks.[24,25] Chronic vocal fold scar is characterized by excessive deposition of disorganized collagen type I.[23,25] Collagen type III is abundant throughout the normal human vocal fold lamina propria[26] but more concentrated in the deep layer.[27] It tends to be more highly concentrated in dynamic regions of elastic tissues and is thought to play a role in maintaining the structure of the ECM.[27] It was shown in a rat model to be upregulated in response to injury, with its level remaining elevated through 12 weeks post-injury and presumably through the remodeling phase of wound healing.[25] In our current model of vocal fold scarring from laser injury, collagen type I was clearly increased (Fig. 3B), whereas collagen type III was not significantly different from control. Our collagen type III data do not necessarily conflict with the previously reported findings in the rat model, since the authors also noted that “the scores of type III (collagen) in scarred vocal folds showed neither a statistical difference from controls nor a difference among study groups (from 2–12 weeks)”.[25] Elastin, which is present in high concentrations in the intermediate layer of the normal human vocal fold lamina propria and is central to the viscoelasticity of the vocal fold, is known to be fragmented and disorganized in scarred lamina propria.[23,28] Our results showed elastin to be increased in the scarred vocal fold, consistent with other reports.[29]

HA is a major component of vocal fold lamina propria ECM and plays a key role in determining the biomechanical properties of the vocal fold cover.[30] It is also thought to play an important role in early-stage wound healing by acting as a matrix to support and guide fibroblast migration and by minimizing the acute inflammatory response that leads to scar formation.[19] Because of the importance of HA, research efforts have focused on the development of HA-based bioengineered therapeutics to minimize vocal fold scarring and to restore normal lamina propria function.[20,31] In animal models of acute vocal fold injury, HA levels have been shown to be decreased compared to normal between days 1-15 after injury, except for a transient increase at day 5 to a level comparable to pre-injury.[19,24] By 2 months after injury, HA remains reduced[25] or recovers to normal levels.[5,23,28] In the current vocal fold scarring model, HA remains decreased at 4 weeks post-injury, which is consistent with the prior reports. Since this model provides a baseline of decreased HA, it appears suitable for the testing of bioengineered therapeutics aimed to increase HA content in injured vocal folds.

One benefit of using an ablative laser to create vocal fold injury in an animal model is that it may mimic vocal fold scarring in humans caused by certain vocal fold surgeries that employ a laser. Laser surgery has had a long history in the treatment of benign and malignant vocal fold lesions. In particular, transoral laser microsurgery (TLM) using the $CO_2$ laser has gained wide acceptance as a minimally invasive surgical modality for the treatment of laryngeal cancers.[32] While heat transfer to normal tissue abutting tumor is in theory minimized by using a pulsed laser, some degree of thermal damage along the laser incision is inevitably present and likely contributes to scarring.[33] Vocal fold scarring following TLM may therefore be better mimicked using an ablative laser injury model. The Ho:YAG laser and $CO_2$ laser share water as the chromophore, and the healing response to tissue injury induced by both lasers has indeed been shown to be comparable in canine vocal folds.[34] In contrast, the pulsed KTP laser, another commonly used laser in vocal fold surgery, is utilized for its theoretical angioselective rather than ablative properties and induces tissue changes that fully return to normal by 4 weeks in a rat model.[35] The rabbit vocal fold scarring model in the current study is not intended to replicate the effect of the pulsed KTP laser.

There are several limitations to this work. It does not specifically address whether tissue injury caused by cold instruments differs from injury induced by laser. It has not been demonstrated that this model produces scarring resembling that caused by laser injury in human vocal folds. However, our intent was not to develop a model to specifically study thermal injury. The current work is a pilot study to demonstrate the feasibility of an alternative vocal fold scarring model. Larger-scale studies using this model to test lamina propria tissue engineered therapies are underway in our laboratory.

## CONCLUSION

We demonstrate the feasibility of using the Ho:YAG laser to create a vocal fold injury model in the rabbit. An optimal laser energy level was identified to induce lamina propria scarring without extensive muscle deficit. The injured vocal fold showed a histologic profile of ECM constituents that is generally consistent with vocal fold scarring in earlier models. This model may serve as an alternative for studying the effects of novel bioengineered therapies for vocal fold scarring.

## Acknowledgments

We thank Paula Timmons and Karen Pawlowski, PhD, for assistance with the animal experiments.

## References

1. Benninger MS, Alessi D, Archer S, et al. Vocal fold scarring: current concepts and management. Otolaryngol Head Neck Surg. 1996; 115:474–482. [PubMed: 8903451]
2. Long JL. Tissue engineering for treatment of vocal fold scar. Curr Opin Otolaryngol Head Neck Surg. 2010; 18:521–525. [PubMed: 20842033]
3. Kutty JK, Webb K. Tissue engineering therapies for the vocal fold lamina propria. Tissue Eng Part B Rev. 2009; 15:249–262. [PubMed: 19338432]

4. Bless DM, Welham NV. Characterization of vocal fold scar formation, prophylaxis, and treatment using animal models. Curr Opin Otolaryngol Head Neck Surg. 2010; 18:481–486. [PubMed: 20962643]
5. Thibeault SL, Gray SD, Bless DM, Chan RW, Ford CN. Histologic and rheologic characterization of vocal fold scarring. J Voice. 2002; 16:96–104. [PubMed: 12002893]
6. Thibeault SL, Klemuk SA, Chen X, Quinchia Johnson BH. In Vivo engineering of the vocal fold ECM with injectable HA hydrogels-late effects on tissue repair and biomechanics in a rabbit model. J Voice. 2011; 25:249–253. [PubMed: 20456912]
7. Svensson B, Nagubothu SR, Cedervall J, et al. Injection of human mesenchymal stem cells improves healing of vocal folds after scar excision--a xenograft analysis. Laryngoscope. 2011; 121:2185–2190. [PubMed: 21898432]
8. Hirano S, Bless DM, Rousseau B, et al. Prevention of vocal fold scarring by topical injection of hepatocyte growth factor in a rabbit model. Laryngoscope. 2004; 114:548–556. [PubMed: 15091233]
9. Hong SJ, Lee SH, Jin SM, et al. Vocal fold wound healing after injection of human adipose-derived stem cells in a rabbit model. Acta Otolaryngol. 2011; 131:1198–1204. [PubMed: 21732743]
10. Suehiro A, Bock JM, Hall JE, Garrett CG, Rousseau B. Feasibility and acute healing of vocal fold microflap incisions in a rabbit model. Laryngoscope. 2012; 122:600–605. [PubMed: 22253007]
11. Liang Q, Liu S, Han P, et al. Micronized acellular dermal matrix as an efficient expansion substrate and delivery vehicle of adipose-derived stem cells for vocal fold regeneration. Laryngoscope. 2012; 122:1815–1825. [PubMed: 22565636]
12. Gleich LL, Rebeiz EE, Pankratov MM, Shapshay SM. The holmium:YAG laser-assisted otolaryngologic procedures. Archives of otolaryngology--head & neck surgery. 1995; 121:1162–1166. [PubMed: 7546585]
13. Fong M, Clarke K, Cron C. Clinical applications of the holmium:YAG laser in disorders of the paediatric airway. The Journal of otolaryngology. 1999; 28:337–343. [PubMed: 10604163]
14. Mau T, Muhlestein J, Callahan S, Weinheimer KT, Chan RW. Phonation threshold pressure and flow in excised human larynges. Laryngoscope. 2011; 121:1743–1751. [PubMed: 21792964]
15. Xu CC, Chan RW, Weinberger DG, Efune G, Pawlowski KS. Controlled release of hepatocyte growth factor from a bovine acellular scaffold for vocal fold reconstruction. J Biomed Mater Res A. 2010; 93:1335–1347. [PubMed: 19876951]
16. Xu CC, Chan RW, Weinberger DG, Efune G, Pawlowski KS. A bovine acellular scaffold for vocal fold reconstruction in a rat model. J Biomed Mater Res A. 2010; 92:18–32. [PubMed: 19165789]
17. Welham NV, Montequin DW, Tateya I, Tateya T, Choi SH, Bless DM. A rat excised larynx model of vocal fold scar. J Speech Lang Hear Res. 2009; 52:1008–1020. [PubMed: 19641079]
18. Kojima T, Mitchell JR, Garrett CG, Rousseau B. Recovery of vibratory function after vocal fold microflap in a rabbit model. Laryngoscope. 2013
19. Thibeault SL, Rousseau B, Welham NV, Hirano S, Bless DM. Hyaluronan levels in acute vocal fold scar. Laryngoscope. 2004; 114:760–764. [PubMed: 15064637]
20. Bartlett RS, Thibeault SL, Prestwich GD. Therapeutic potential of gel-based injectables for vocal fold regeneration. Biomed Mater. 2012; 7:024103. [PubMed: 22456756]
21. Thibeault SL, Duflo S. Inflammatory cytokine responses to synthetic extracellular matrix injection to the vocal fold lamina propria. Ann Otol Rhinol Laryngol. 2008; 117:221–226. [PubMed: 18444483]
22. Lin Y, Yamashita M, Zhang J, Ling C, Welham NV. Pulsed dye laser-induced inflammatory response and extracellular matrix turnover in rat vocal folds and vocal fold fibroblasts. Lasers Surg Med. 2009; 41:585–594. [PubMed: 19746432]
23. Rousseau B, Hirano S, Chan RW, et al. Characterization of chronic vocal fold scarring in a rabbit model. J Voice. 2004; 18:116–124. [PubMed: 15070231]
24. Tateya T, Tateya I, Sohn JH, Bless DM. Histological study of acute vocal fold injury in a rat model. Ann Otol Rhinol Laryngol. 2006; 115:285–292. [PubMed: 16676825]
25. Tateya T, Tateya I, Sohn JH, Bless DM. Histologic characterization of rat vocal fold scarring. Ann Otol Rhinol Laryngol. 2005; 114:183–191. [PubMed: 15825566]

26. Tateya T, Tateya I, Bless DM. Collagen subtypes in human vocal folds. Ann Otol Rhinol Laryngol. 2006; 115:469–476. [PubMed: 16805380]
27. Hahn MS, Kobler JB, Zeitels SM, Langer R. Quantitative and comparative studies of the vocal fold extracellular matrix II: collagen. Ann Otol Rhinol Laryngol. 2006; 115:225–232. [PubMed: 16572613]
28. Rousseau B, Hirano S, Scheidt TD, et al. Characterization of vocal fold scarring in a canine model. Laryngoscope. 2003; 113:620–627. [PubMed: 12671417]
29. Lim JY, Choi BH, Lee S, Jang YH, Choi JS, Kim YM. Regulation of wound healing by granulocyte-macrophage colony-stimulating factor after vocal fold injury. Plos One. 2013; 8:e54256. [PubMed: 23372696]
30. Chan RW, Gray SD, Titze IR. The importance of hyaluronic acid in vocal fold biomechanics. Otolaryngol Head Neck Surg. 2001; 124:607–614. [PubMed: 11391249]
31. Gaston J, Thibeault SL. Hyaluronic acid hydrogels for vocal fold wound healing. Biomatter. 2013; 3
32. Rubinstein M, Armstrong WB. Transoral laser microsurgery for laryngeal cancer: a primer and review of laser dosimetry. Lasers in medical science. 2011; 26:113–124. [PubMed: 20835840]
33. Reinisch L, Garrett CG, Courey M. A simplified laser treatment planning system: proof of concept. Lasers Surg Med. 2013; 45:679–685. [PubMed: 24249302]
34. Kay SL, Oz MC, Haber M, Blitzer A, Treat MR, Trokel SL. Soft tissue effects of the THC:YAG laser on canine vocal cords. Otolaryngol Head Neck Surg. 1992; 107:438–443. [PubMed: 1408232]
35. Mallur PS, Branski RC, Amin MR. 532-nanometer potassium titanyl phosphate (KTP) laser-induced expression of selective matrix metalloproteinases (MMP) in the rat larynx. Laryngoscope. 2011; 121:320–324. [PubMed: 21271581]

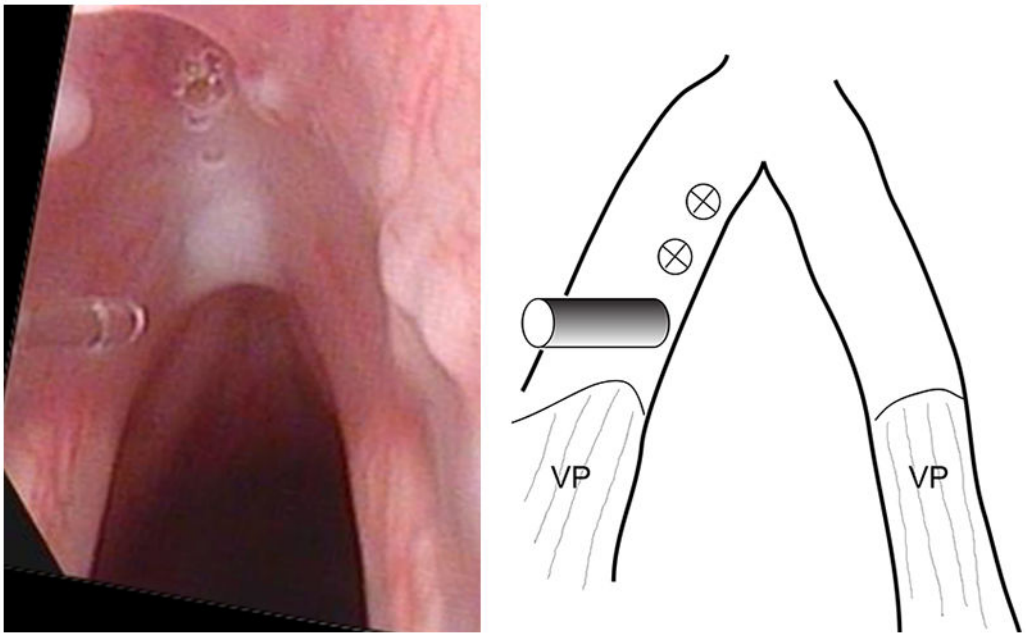


**Figure 1.**

Intraoperative photo of the Ho:YAG fiber in contact with the left vocal fold mucosa (left panel), and schematic showing the locations of laser application (right panel). The fiber is positioned at the most posterior of the 3 locations of laser application, and the two anterior ones are marked in the schematic. VP – vocal process.

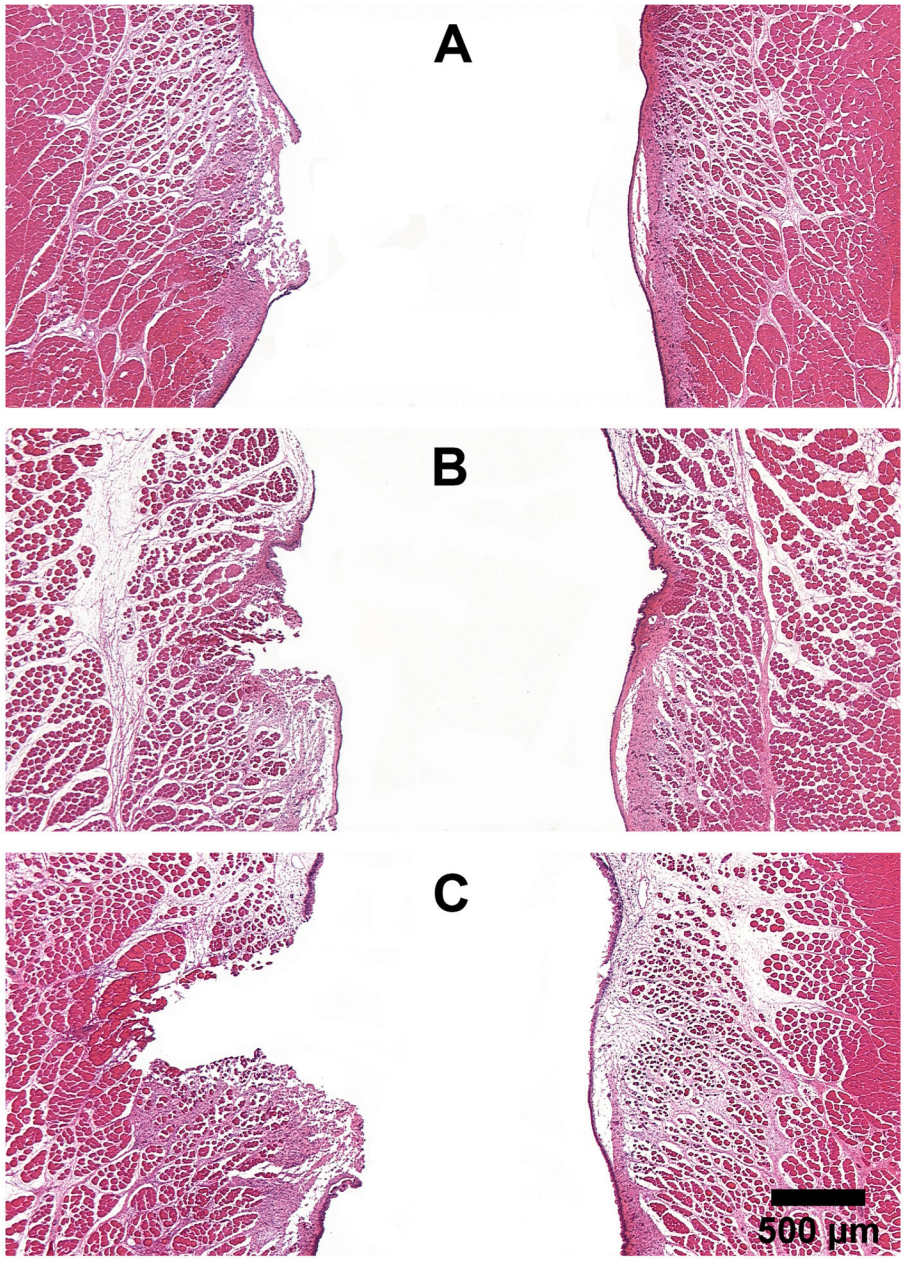


**Figure 2.**

Histological coronal sections of rabbit larynges stained with H&E, showing the extent of injury immediately after laser application at various energy levels: (A) 0.6 J, (B) 1.8 J, and (C) 3.0 J. Vocal fold on left - laser injury; right - normal. (25X)

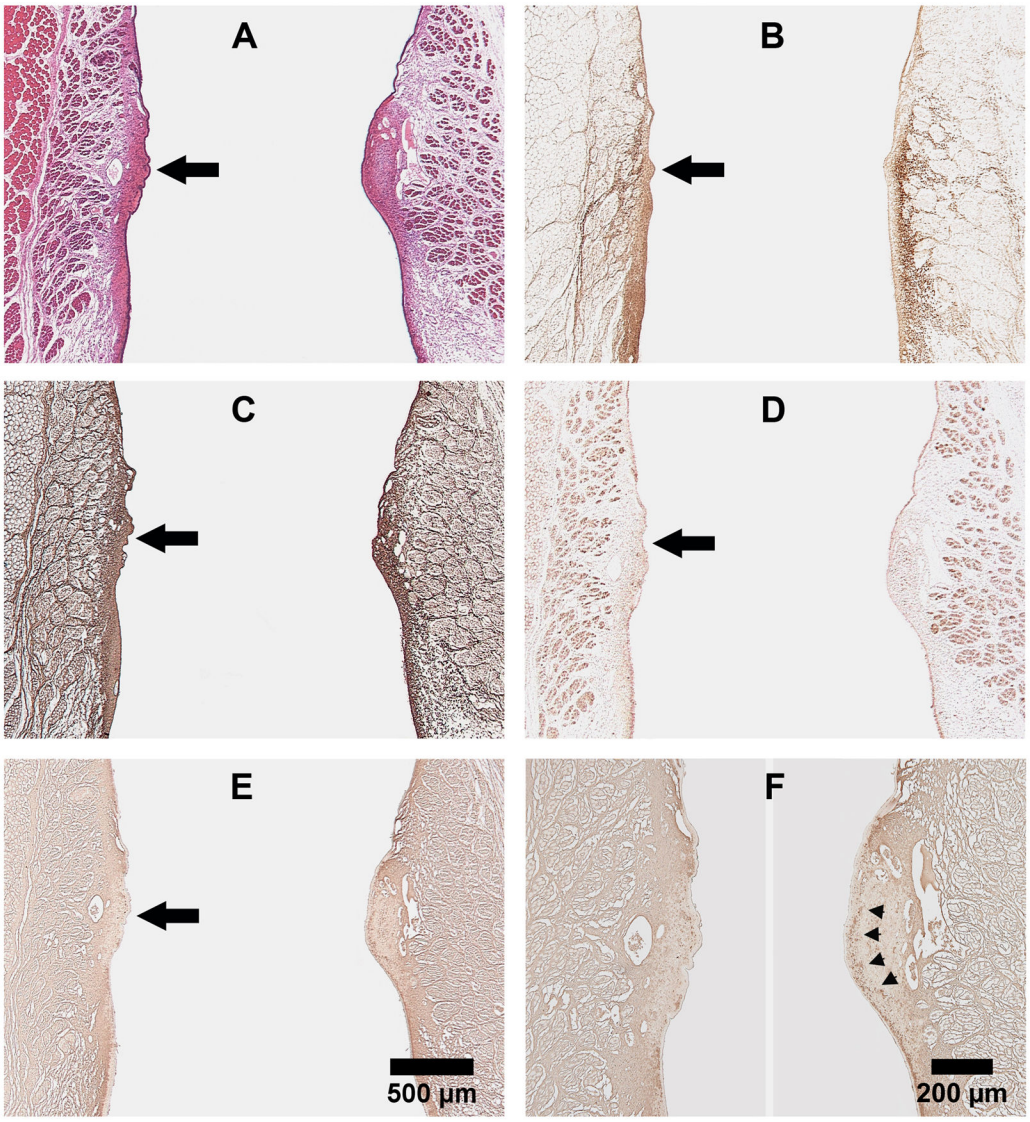


**Figure 3.**

Representative coronal sections of rabbit larynges harvested 4 weeks after laser treatment. (A) H&E; (B) Collagen type I; (C) Collagen type III; (D) Elastin; and (E) Hyaluronic acid. Vocal fold on left - scarred; right - normal. Panels A-E (25X): Large black arrow points to the location of laser injury. (F) Higher magnification of (E), with arrowheads pointing to the continuous band of HA in the lamina propria of normal vocal fold (100X).

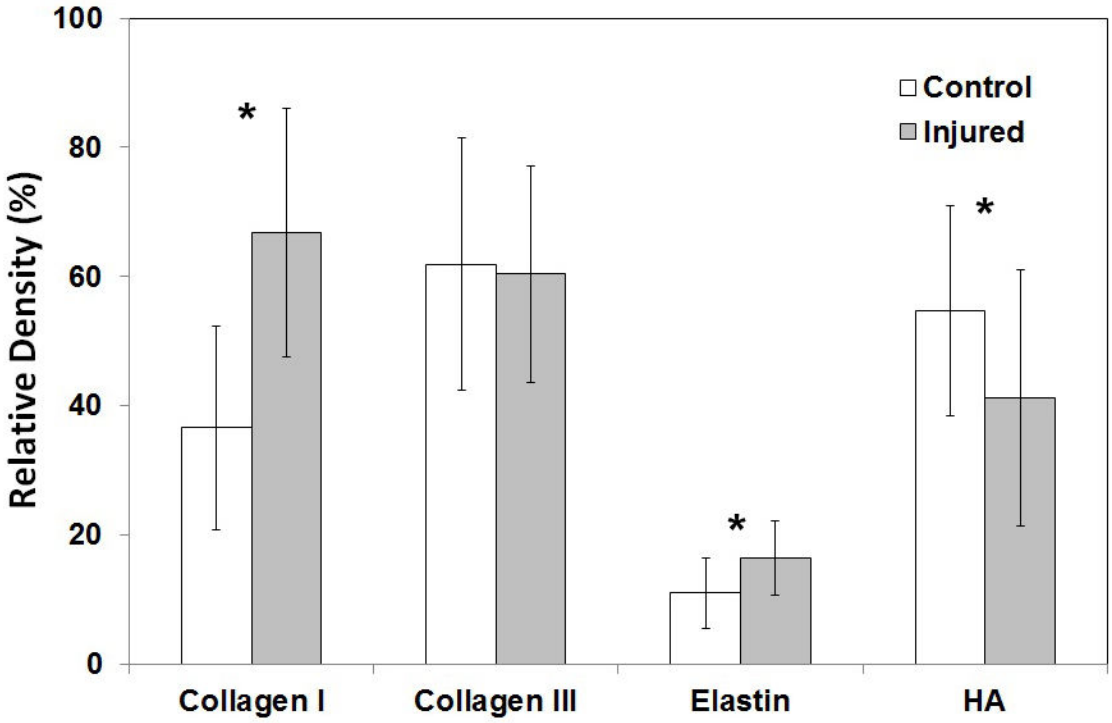


**Figure 4.**

Relative densities of ECM constituents in IHC staining in normal vs. scarred rabbit vocal folds 4 weeks after laser treatment ($n = 8$). *$P < 0.05$ for differences between the two groups.

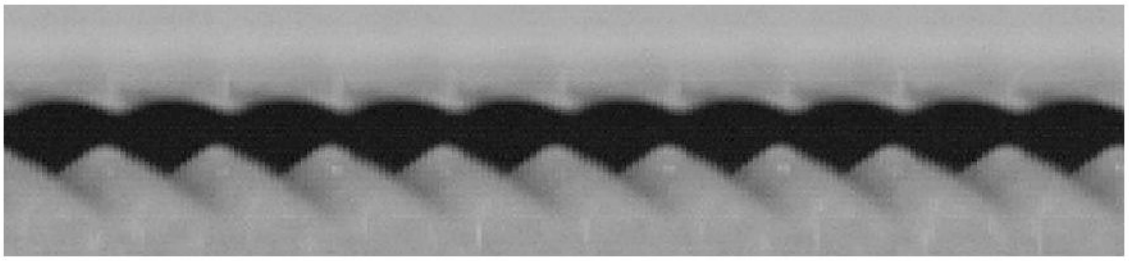

**Figure 5.**
A representative videokymograph from high-speed imaging of excised larynx phonation with scarred left vocal fold (top) and normal right vocal fold (bottom).